

Numerical Investigation of Phase-Change Heat Transfer for Laser-Assisted Direct Nano Imprint Processing

Fei-Bin Hsiao¹, Di-Bao Wang¹ and Chun-Ping Jen¹, Yung-Chun Lee² and Cheng-Hsin Chuang³

¹Institute of Aeronautics and Astronautics, National Cheng Kung University, Tainan, Taiwan

²Department of Mechanical Engineering, National Cheng Kung University, Tainan, Taiwan

³Electronics Research & Service Organization, Industrial Technology Research Institute, Hsinchu, Taiwan

¹ Person to Contact: fbhsiao@mail.ncku.edu.tw

ABSTRACT

The melting duration and molten depth are key information for Laser-Assisted Direct Imprinting, which raises the issue of the melting & solidification induced by excimer-pulse-laser shining through unilaterally transparent binary materials. Based on the matured laser-annealing analysis, the thermal-contact resistance is taken into account to simulate and predict the melting behavior for this process. The result in this study indicates the laser-annealing case as well as the perfect-contact case provide the upper-bound and the lower-bound values for the physical quantities involved in this process even without the detail information of the changing of thermal-contact resistance during process.

Keywords: nano imprint, pulsed laser, heat conduction, phase change, thermal-contact resistance

1 INTRODUCTION

Nano-imprinting lithography (NIL) has been developed over a decade and is a promising method of nano-patterning and nano-fabrication. Since 2002, a novel technique called Laser-Assisted Direct Imprinting (LADI) method has been proposed to utilize an excimer laser to irradiate and then heat the silicon surface through a highly-transparent quartz mold preloaded onto the silicon [1]. However, this new method raises engineering challenges such as the optimized combination of laser parameters as well as preloading pressures which are deemed crucial to the future applications. For instance, the molten depth and melting duration are the key issues regarding the deformation and stress-propagation of both silicon substrate and quartz mold during imprinting. Therefore the main purpose of the present study is to develop a numerical program for predicting the required information for the LADI fabrication.

As illustrated in Figure 1, the heat-transfer topic faced by the LADI process is the melting/solidification induced by excimer-pulse-laser shining through

unilaterally-transparent binary materials. In the past two decades, laser-induced melting of single material has been investigated by many researchers, however, for LADI process not only the laser-annealing but also the heat-flux between two materials (silicon and quartz) should be taken into account. As a result, the thermal-contact resistance between two materials plays an important role in predicting the temperature field, melting duration and molten depth for this process, which would be the main purpose of this study.

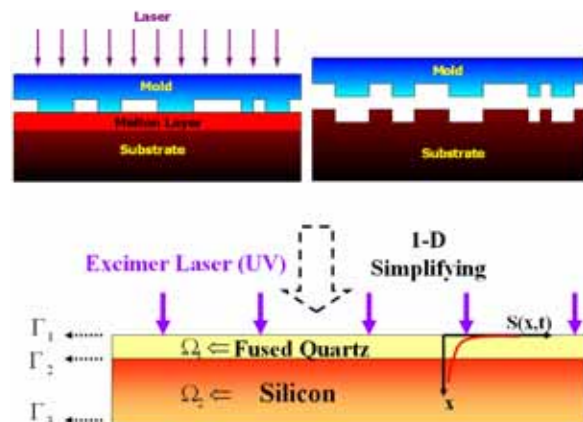


Fig.1. Illustration of LADI imprinting process and one-dimensional simplification

2 GOVERNING EQUATION AND NUMERICAL ALGORITHM

The heat-transfer system discussed here consists of two materials (Ω_1 and Ω_2) contacting with each other. Irradiated from above, the excimer-laser (ultraviolet) travels without absorption through Ω_1 and next arrives at the surface of Ω_2 with exponentially-decaying absorption therein as illustrated in Figure 1. Since the characteristic time for lattice vibration is about the magnitude of pico-second, the concept of thermodynamic coefficients (C and T) and thermal-transport coefficients (K) could make physical sense in time scale of nano-second. Therefore, the

continuum-based description of heat conduction is still valid for laser heating with pulse duration of several decades in nano-second.

Including the heat-source induced by absorption of excimer-laser, the equation of heat transport within two materials in one-dimension could be written as

$$\rho C(T) \frac{\partial T(x,t)}{\partial t} = \frac{\partial}{\partial x} \left[K(T) \frac{\partial T(x,t)}{\partial x} \right] + S(x,t) \quad (1)$$

$$x \in \Omega_1 \cup \Omega_2$$

where ρ, K, C, T and S represent density, thermal conductivity, specific heat capacity, temperature and heat-source term respectively. The heat-source term $S(x,t)$ (W/cm^3) can be further written as

$$S(x,t) = I(t) \cdot \alpha \cdot (1 - R) \cdot \exp[-\alpha(x - x_0)], \quad (2)$$

where $I(t)$ (W/cm^2) describes the pulse-shape of laser, α (cm^{-1}) represents the absorption coefficient, R is the reflectivity of the light irradiating on material and x_0 is the position for which the material starts to absorb the laser energy. If x_0 is not melted yet, the value of x_0 remains zero; however, x_0 will be negative while x_0 is melted. Usually $I(t)$ and α is pre-assumed or derived from experimental measurement in order to perform the computation.

There are three boundaries to be dealt with in this study. The right-hand-side of Ω_2 is imposed the Dirichlet boundary condition while the other two are imposed the Neumann boundary conditions. As shown in Figure 1, conditions at three boundaries $\Gamma_1 \sim \Gamma_3$ are described as

$$\begin{cases} \Gamma_1 : & q'' = 0 \\ \Gamma_2 : & q'' = -\frac{\Delta T}{R''} \\ \Gamma_3 : & T = T_0 \end{cases} \quad (3)$$

where q'' (W/m^2) is the heat-flux per unit area, R'' (m^2-K/W) is the thermal-contact resistance and T_0 is the room or initial temperature. For its small order of magnitude compared with heat flux, the thermal radiation at Γ_1 is neglected.

As for the modeling of melting phase-change of both materials, the present study is not going to calculate the position and velocity of the moving solid-liquid interface as most researchers do, but rather adopts a straightforward way --- the enthalpy formulation. This method replaces the discontinuous change in the enthalpy-temperature diagram by a deep but continuous curve in the narrow neighborhood of the melting temperature. Besides, the melting phase-change will

increase the absorption coefficient as well as the reflectivity parameter [2]. For simplicity, both values are switched while phase-change occurs.

With known dependence on time, spatial and temperature for specific heat-capacity, thermal conductivity and heat-source term for both materials (see Figure 2), the transient spatial distribution of temperature $T(x,t)$ is then solved by explicit finite-difference-method in this study. Since the grid-width is exponentially dense near boundaries and interfaces, namely the grid-width is not constant, the iteration algorithm for each grid at each time-step will be

$$T_i^n = T_i^{n-1} + \frac{S_i^n \Delta t}{C_i} + \frac{\Delta t}{\Delta x_i (\Delta x_i + \Delta x_{i+1})} \frac{(K_{i+1} + K_i)(T_{i+1}^{n-1} - T_i^{n-1})}{C_i} - \frac{\Delta t}{\Delta x_i (\Delta x_{i-1} + \Delta x_i)} \frac{(K_i + K_{i-1})(T_i^{n-1} - T_{i-1}^{n-1})}{C_i} \quad (4)$$

$$i = 1 \sim N, n = 1 \sim M$$

where N and M are numbers of grids and time-steps, and Δx_i is the grid-width of each grid. For each computation case in this study, the initial temperature of all domains is given as room temperature (300 K) and the laser pulse is triggered at $t = 0$.

The thermal-contact resistance, R'' , actually dominates the temperature response and the melting behavior of both materials. In order to understand the effect of thermal-contact resistance, this study first investigates the basic case with infinite resistance at the interface, that is, no heat-flux across two materials and hence this case is equivalent to laser-annealing on single material. Next, the case with finite and zero thermal-contact resistance will also be discussed and compared with the first case. In the following discussion, fused quartz and crystalline silicon will represent Ω_1 and Ω_2 respectively for the main purpose of this study.

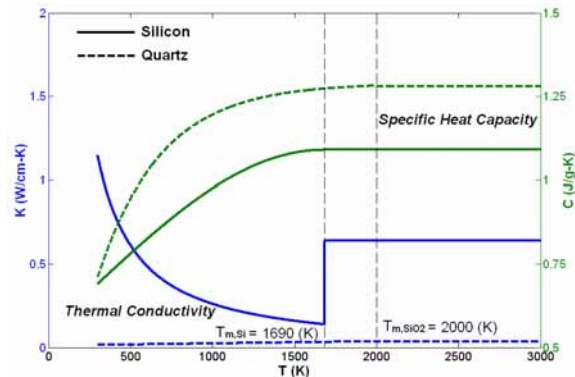


Fig.2 Variation of thermal conductivity and specific heat capacity with respect to temperature for silicon and quartz. temperature ranges from 300 to 3000 K

3 RESULTS AND DISCUSSIONS

In the following discussion, the variation of thermal conductivity and specific capacity for silicon and quartz is referred and curve-fitted for simulation program as plotted in Figure 2. The melting temperatures of silicon and quartz are chosen to be 1690 K and 2000 K in this study. Each case takes the KrF excimer laser ($\lambda = 248\text{-nm}$, FWHM = 30 ns, fluence = $0 \sim 1.5 \text{ J/cm}^2$) as the laser model and assumes the pulse shape to be a Gaussian-typed distribution.

3.1 Infinite Thermal-Contact Resistance

The time-history of the molten depth of silicon for laser fluence ranging from 0.4 to 1.4 (J/cm^2) is shown in Figure 3 and it can be seen that larger fluence could cause faster melting speed and deeper molten depth. However, it can also be observed that larger fluence seems to have little influence on the resolidification speed, which averages about 5 (m/s) for each influence. Since the resolidification speed larger than 15 (m/s) will result in the amorphization of the silicon [3] and hence the governing equation in this study doesn't have to model the transfer of crystal type. Compared with the referred experimental data [3,4,5] as shown in Figure 4, it can be seen that the simulation result of the present study agrees with the measurement in tendency and the order of magnitude. Since the pulse durations of the three data are not the same, the molten depths should be different. Even with the same pulse duration, there still be unavoidable discrepancy, which would be due to the exact values of reflectivity and the absorption coefficient during the melting and resolidification process; however, these two values dominate the amount of absorbed photon energy and its range of spatial distribution.

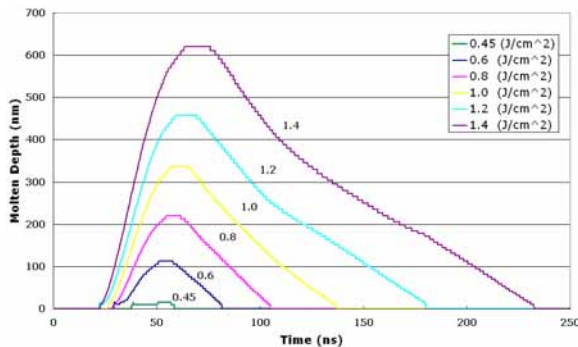


Fig.3 Simulation result for the time response of molten depth of crystalline-silicon under illumination of krf excimer laser with fluence from 0.45 to 1.4 (J/cm^2).

Figure 5 shows the general observation for the effect of laser fluence on the molten depth, melting duration and the maximum surface-temperature. As a whole, larger fluence results in deeper molten depth, longer

melting duration, faster melting/resolidification speed and larger maximum surface-temperature as expected. According to the present result, the threshold of laser fluence for silicon substrate under the laser type and conditions mentioned above is about $0.4 \text{ (J/cm}^2\text{)}$. Next, the effect of quartz-contact to silicon during laser heating is going to be discussed.

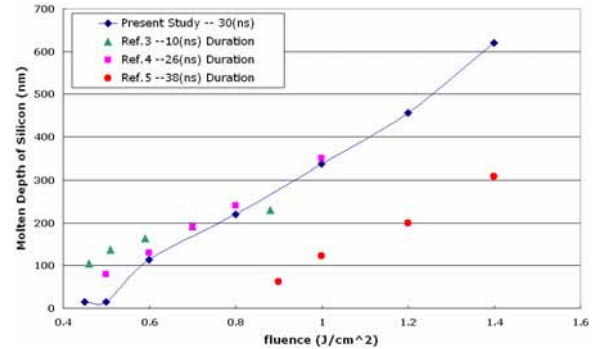


Fig.4 Simulation and referred experimental results for the maximum molten depth of crystalline-silicon with various laser fluence and pulse duration

3.2 Zero Thermal-Contact Resistance

In order to take the first glance of the effect of quartz-contact onto silicon, the perfect-contact case ($R'' = 0$) is considered herein as the extreme example. Since the existence of quartz in contact with silicon provides another outlet for the heat from the hot silicon, the thermal effect from laser-heating onto the silicon is reduced. Figure 5 illustrates that the excimer laser heating the silicon through the contacting quartz may results in, as expected, lower maximum temperature of silicon, shallower maximum molten depth of silicon and shorter melting duration of silicon compared with the case of silicon only. Perfect contact means no temperature difference between silicon and quartz, therefore the upper plot of Figure 8 indicate the quartz may over its melting point (2000 K), which is also witnessed where the quartz is melted by the ambient silicon when the fluence is high enough (in this study, 1.2 J/cm^2). Also, the melting threshold of fluence increases up to $0.8 \text{ (J/cm}^2\text{)}$ here. However, what's mentioned in this paragraph may not be true since there are no two materials contacting with each other have zero thermal-contact resistance in real world.

3.3 Finite Thermal-Contact Resistance

Generally speaking, the value of the thermal-contact resistance between two materials is about 10^{-4} to $10^{-5} \text{ (m}^2\text{-K/W)}$ [6]. However, the detail information of the thermal-contact resistance between silicon and quartz is hard to obtained for such a large variation range of temperature, say, $300 \text{ K} \sim 2500 \text{ K}$; the melting and

resolidification phase-change make the modeling even worse. For instance, when silicon melts the joint with quartz may be enhanced and then lower the thermal-contact resistance between. Although how the thermal-contact resistance changes during the rising of temperature and melting of materials is not exactly known, the influence of it still could be unveiled by testing various values for fixed fluence (assuming that such resistance remains constant).

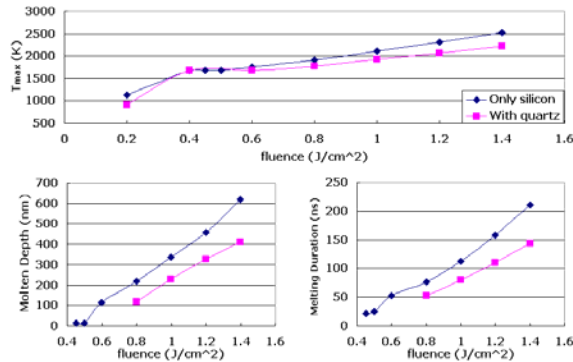


Fig.5 Effect of fluence on the maximum surface temperature, molten depth, and melting duration of silicon for the case of silicon only and the case with contacting quartz

Taking fluence of 1.0 (J/cm²) as the standard case, thermal-contact resistance of 10⁻³ to 10⁻¹⁰ (m²-K/W) is tested to observe its effect on the molten depth, melting duration of silicon and the maximum surface temperature of silicon & quartz as shown in Figure 6. In this figure, it is seen that each physical quantity (molten depth, melting duration & maximum surface temperature) approaches its limiting value on both sides of the axis of R'' . Compared with Figure 5, it is further found that these limiting constants are just the values of the case of only silicon and the case of perfect contact. Actually, there exist four kinds of situation for the quartz to contact with silicon depending on the thermal-contact resistance:

- (I) $R'' \gg 1$ (equivalent to only-silicon case).
 - (II) R'' remains constant during the whole process.
 - (III) R'' approaches zero gradually as the surface temperature rises and melting occurs.
 - (IV) R'' equals zero all the time (perfect-contact case).
- Based on the definition of R''

$$R'' \equiv \left| \frac{\Delta T}{q''} \right|, \quad (5)$$

it is easy to know that the order of extent of thermal effect onto silicon with quartz-contact for these four situation would be (I) > (II) > (III) > (IV) because the larger the R'' is, the less heat would flow out from the silicon. This order is also guaranteed by the simulation for case (II) which shows deeper depth, longer duration and larger temperature than case (III); besides, both cases are bounded by case (I) as well as case (IV). Therefore, it

is concluded that no matter what the thermal-contact resistance is or how the thermal-contact resistance varies, Figure 5, namely case (I) and (II), provides upper and lower limit for the molten depth, melting duration of silicon as well as the maximum surface temperature of silicon & quartz.

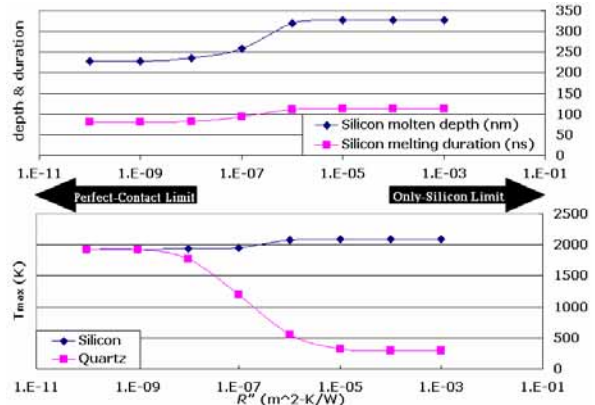


Fig.6 Effect of thermal-contact resistance on molten depth, melting duration of silicon and maximum surface temperature of silicon & quartz with laser fluence of 1.0 (j/cm²)

4 CONCLUSION

Considering the melting/solidification of silicon surface induced by excimer-pulse-laser shining through quartz contacting with the silicon, this study successfully takes the cooling effect from quartz as well as the thermal-contact resistance between two materials to formulate the physical model and to perform its numerical simulation.

Combining all tested cases, it is found that no matter what the thermal-contact resistance is or how the thermal-contact resistance varies the only-silicon case and perfect-contact case together provide upper and lower limit for the molten depth, melting duration of silicon as well as the maximum surface temperature of silicon & quartz.

REFERENCES

- [1] Chou, S.Y., Keimei, C. and Gu, J., *Nature*, 417, pp.835-837 (2002).
- [2] Wood, R.F. and Giles, G.E., *Phys. Rev. B*, Vol.23, No.6, 2923-2942, 1981
- [3] Thompson, M.O. et al, *Phys. Rev. Lett.*, Vol.50, No.12, 896-899, 1983
- [4] Jellison, G.E. et al, *Phys. Rev. B*, Vol.34, No.4, 2407-2415, 1986
- [5] Xu, X., Grigoropoulos, C.P., and Russo, R.E., *Appl. Phys. A*, Vol.62, 51-59, 1996
- [6] Incropera, F.P. and DeWitt, D.P., *Fundamentals of Heat and Mass Transfer*, 4th edition, pp.80-81, 1996